Memorias del 2023 Congreso Nacional de Control Automático
25-27 de Octubre, 2023. Acapulco, Guerrero, México.

Sliding Mode Observer Design for Fault Estimation in Cardiovascular System

Dulce-A. SERRANO-CRUZ [*, **] **Latifa BOUTAT-BADDAS** [*] **Mohamed DAROUACH** [*], **Carlos-M. ASTORGA-ZARAGOZA** [**], **and Gerardo-V. GUERRERO-RAMÍREZ** [**]

[*] *CRAN, UMR 7039, Université de Lorraine, IUT de Longwy, 186, Rue de Lorraine, 54400 Cosnes et Romain, France, (e-mail: alejandra.serrano17ee@cenidet.edu.mx and {latifa.baddas, mohamed.darouach}@univ-lorraine.fr).*
[**] *Tecnologico Nacional de México, CENIDET, Cuernavaca, Mor., C.P.62490, (e-mail: {astorga, gerardo.gr}@cenidet.tecnm.mx).*

Abstract:
This paper deals with the design of a sliding mode observer allowing to estimate the state vector of a nonlinear dynamical cardiovascular system linearly unobservable. This state estimation is used for detecting faults to study the problem of cardiovascular anomalies that can originate from variations in physiological parameters and deviations in the performance of the heart's mitral and aortic valves.

Keywords: Cardiovascular system, normal form, sliding modes, unobservable states,

1. INTRODUCTION

Cardiovascular diseases (CVDs) continue to be the leading cause of death worldwide (Organization (June 2023)). Therefore, many studies have been devoted to modeling the CVS to well understand its behavior and to find new reliable diagnosis techniques (Traver et al. (2022), Ledezma and Laleg-Kirati (2012), Laleg-Kirati et al. (2015), Fónod and Krokavec (2012)). Mathematical models have emerged as valuable tools, offering simpler and less expensive experiments compared to in vitro heart experiments [Korakianitis and Shi (2006), Simaan (2008), Ferreira et al. (2005), Traver et al. (2022)].
Fault detection and localization methods for systems represented using a dynamic model include those based on the generation of fault indicators (often called residuals) calculated as the difference between measurements taken on the real system and estimates calculated by an observer. Numerous results based on linear models in particular have been published in a variety of situations. However, when we wish to represent the behavior of a system using a nonlinear model, the design of observers is generally more delicate. For nonlinear systems, observability analysis, there are no simple general techniques to design an observer for all types of nonlinear systems. In this paper, we use the cardiovascular system model as introduced by Simaan (2008), Ledezma and Laleg-Kirati (2012), and Belkhatir et al. (2014). We propose a methodology for detecting faults, aiming to address the challenge of identifying cardiovascular anomalies that may arise because of variations in physiological parameters and irregularities in the heart's performance's mitral and aortic valves. The SCV model presents two principal difficulties: First, the SCV system has a hybrid aspect due a natural consequence of the presence of valves (aortic and mitral). Depending on the open or closed state of these valves, the cardiac cycle is divided into four operating modes. Second, the linear part of the model SCV is not observable (Krener and Isidori (1983), Boutat-Baddas (2002) and Serrano-Cruz et al. (2021)) (i.e. does not respect Brunovsky's observability rank criterion (Brunovskỳ (1970)). In this paper, we consider the observer design problem for state estimation in the cardiovascular system and to take full advantage of the structural properties of the system, our idea is to design a sliding mode observer, that allows us to solve the problems of observability singularities [Boutat-Baddas (2002) and Serrano-Cruz et al. (2021)].
Sliding-mode observers use techniques based on variable-structure or sliding-mode system theory (see Drazenovic (1969), Utkin (1977), Utkin (1992)). The sliding-mode observer is an observer whose correction term is a sign function. The principle comprises of using discontinuous functions to force the dynamics of observation errors to converge towards a variety known as the sliding surface. The attractiveness of this surface is ensured by conditions called slip conditions, the dynamics of which are computed using the equivalent ordering method (see Drakunov (1992), Drakunov and Utkin (1995)). A so-called step-by-step convergence strategy is performed to ensure convergence of each state variable one after the other in finite time (see Barbot et al. (2002), Floquet and

Barbot (2007), Barbot and Floquet (2010), Y. Shtessel and Levant (2014)). One of the main features of these observers is their robustness against external disturbances and modeling errors or system uncertainties, in addition to the property of fast, finite-time convergence of observation errors.

The paper is organized as follows, in section 2 we will present a briefly describes the considered nonlinear model of the cardiovascular system and after an analysis of the observability of the cardiovascular system, we will present a sliding modes observer design. Section 3, the CVS model for detection of anomalies is presented and 2 types of faults in the mitral and aortic valves are considered, based on the obtained results, some simulation results are presented to show how this design has the ability to estimate system states to monitor the activity cardiovascular. Finally, section 4 presents the conclusions.
.

2. OBSERVABILITY ANALYSIS AND OBSERVER DESIGN OF THE CARDIOVASCULAR SYSTEM

2.1 Presentation of the cardiovascular system

Let us consider the cardiovascular system presented in Diaz Ledezma and Laleg-Kirati (2015) and Simaan et al. (2008):

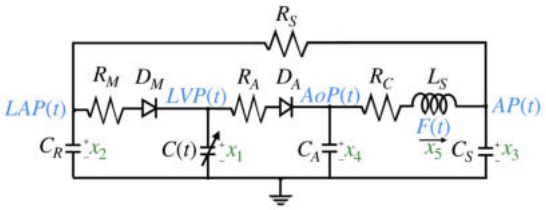

Fig. 1. Model of the cardiovascular system.

In this model, voltages are analogous to pressure and currents are analogous to blood. The circuit model in Figure 1 represents the heart's left ventricle hemodynamics. This model comprises the following parts:

1) Preload: is represented by the pulmonary circulation and the heart left atrium are represented are represented by the capacitance, C_R; the mitral valve is represented by resistor R_M and ideal diode D_M; the aortic valve is represented by resistor R_A and ideal diode D_A; a fourth capacitor is introduced to account for the compliance of the aorta C_A.
2) Afterload: is represented by the systemic circulation is modeled as a four-element Windkessel model comprising (R_C, L_C, R_S, C_S).

The left ventricle is represented by a time-varying compliance $C(t)$, which is the inverse of the ventricle's elastance function $E(t)$. The behavior of the left ventricle is modeled as $C(t) = \frac{1}{E(t)}$, where $E(t)$ is relates to the ventricle's pressure and volume according to an expression of the form $E(t) = (E_{max} - E_{min})E_n(t_n) + E_{min}$ where

$$E_n(t_n) = 1.55\left(\frac{(\frac{tn}{0.7})^{1.9}}{1+(\frac{tn}{0.7})^{1.9}}\right)\left(\frac{1}{1+(\frac{tn}{1.17})^{21.9}}\right) \quad (1)$$

$E_n(t_n)$ is the normalized elastance, $t_n = t/(0.2{+}0.15\frac{60}{H_R})$, with H_R is the heart rate expressed in beats per minute (bpm), $E_{max} = 2$ and $E_{min} = 0.06\ mmHg/ml$. Let the vector $u(t) \in \mathbb{R}^2$ be the natural input vector representing the mitral valve D_M and aortic valve D_A given by:

$$D_M = \begin{cases} 0, & x_2 < x_1 \\ 1, & x_2 \geq x_1 \end{cases}, D_A = \begin{cases} 0, & x_1 < x_4 \\ 1, & x_1 \geq x_4 \end{cases} \quad (2)$$

where D_M and D_A are the control inputs sequence of the system. Table 1 shows the system parameters.

Table 1. Physiological meaning of the model

variables	name	Physiological parameter
$x_1(t)$	LVP(t)	Left ventricular pressure (mmHg)
$x_2(t)$	LAP(t)	Left atrial pressure (mmHg)
$x_3(t)$	AP(t)	Arterial pressure (mmHg)
$x_4(t)$	$A_o(t)$	Aortic pressure (mmHg)
$x_5(t)$	F(t)	aortic flow (ml/s)

Now, we present the equations of this system are defined by the following model:

$$\begin{cases} \dot{x}_1 = \frac{-\dot{C}(t)}{C(t)}x_1 - \frac{D_M}{C(t)R_M}(x_1 - x_2) - \frac{D_A}{C(t)R_A}(x_1 - x_4) \\ \dot{x}_2 = \frac{1}{R_S C_R}(x_3 - x_2) + \frac{1}{C_R R_M}(x_1 - x_2)D_M \\ \dot{x}_3 = \frac{1}{R_S C_S}(x_2 - x_3) + \frac{1}{C_S}x_5 \\ \dot{x}_4 = -\frac{1}{C_A}x_5 + \frac{1}{C_A R_A}(x_1 - x_4)D_A \\ \dot{x}_5 = -\frac{1}{L_S}x_3 + \frac{1}{L_S}x_4 - \frac{R_C}{L_S}x_5 \end{cases} \quad (3)$$

with $y_1 = x_5$ and $y_2 = x_4$ are the outputs of CVS. It is important to note that the measurements considered can be obtained non-invasive, thanks to some recent devices: N-point moving average Xiao et al. (2018) and wearable Doppler ultrasound patch Émile S. Kenny (2021).

2.2 Observability analysis

Consider the following change of coordinates:

$$\begin{aligned} z_1^1 &= x_5 \\ z_2^1 &= -\frac{1}{L_S}x_3 \\ z_3^1 &= -\frac{1}{L_S R_S C_S}x_2 + \frac{1}{L_S R_S C_S}x_3 \\ z_1^2 &= x_4 \\ z_2^2 &= C(t)x_1(t) \end{aligned} \quad (4)$$

We obtain directly the quadratic normal form of the CV system, as a result, we have:

$$\begin{cases} \dot{z}_1^1 = -\frac{R_C}{L_S}z_1^1 + z_2^1 + \beta^{12}z_1^2 \\ \dot{z}_2^1 = -\frac{1}{L_S C_S}z_1^1 + z_3^1 \\ \dot{z}_3^1 = \frac{1}{L_S R_S C_S^2}z_1^1 - \beta^{13}z_3^1 - k_{31}^{13}z_3^1 u_1 - k_{21}^{13}z_2^1 u_1 - k_{22}^{13}z_2^2 u_3 \\ \dot{z}_1^2 = \beta^{21}z_1^1 - \frac{1}{C_A R_A}z_1^2 u_2 - \frac{1}{C_A R_A}z_2^2 u_4 \\ \dot{z}_2^2 = k_{31}^{22}z_3^1 u_1 - \frac{L_S}{R_M}z_2^1 u_1 + \frac{1}{R_A}z_1^2 u_2 - \frac{1}{R_M}z_2^2 u_3 - \frac{1}{R_A}z_2^2 u_4 \end{cases} \quad (5)$$

where $\beta^{12} = \frac{1}{L_S}, \beta^{13} = \frac{1}{R_S C_R} + \frac{1}{R_S C_S}, k_{31}^{13} = \frac{1}{C_R R_M}, k_{21}^{13} = \frac{1}{R_S C_S C_R R_M}, k_{22}^{13} = \frac{1}{L_S R_S C_S C_R R_M}, \beta^{21} = \frac{-1}{C_A}, k_{31}^{22} = -\frac{L_S R_S C_S}{R_M},$

and $u_1 = D_M$, $u_2 = D_A$, $u_3 = D_M \frac{1}{C(t)}$ and $u_4 = D_A \frac{1}{C(t)}$.
For the considered cardiovascular system the resonant terms are $k_{22}^{13} z_2^2 u_3$, $k_{22}^{21} z_2^2 u_4$, $k_{22}^{22} z_2^2 u_3$ and $k_{12}^{22} z_2^2 u_4$. As a result, thanks to resonant terms $k_{12}^{21} z_2^2 u_4$ and $k_{23}^{13} u_3 z_2^2$ we can recover the observability for z_2^2.

Now, we will do a structural analysis of observability applied to the CVS model (5). For this, let O the observability matrix given by:

$$O = \left[dy_1, dy_2, dL_f y_1, dL_f y_2, dL_f^2 y_1 \right]^T \tag{6}$$

which gives

$$O = \begin{bmatrix} 1 & 0 & 0 & 0 & 0 \\ 0 & 0 & 0 & 1 & 0 \\ -\frac{R_C}{L_S} & 1 & 0 & \beta^{12} & 0 \\ \beta^{21} & 0 & 0 & \frac{-1}{C_A R_A} u_2 & \frac{-1}{C_A R_A} u_4 \\ M_{11}^1 & -\frac{R_C}{L_S} & 1 & M_{14}^1 & \beta^{12} k_{12}^{21} u_4 \end{bmatrix} \tag{7}$$

where $M_{11}^1 = \frac{R_C^2}{L_S^2} - \frac{1}{L_S C_S} + \beta^{12}\beta^{21}$, $M_{14}^1 = \frac{R_C}{L_S^2} - \frac{\beta^{12} u_2}{C_A R_A}$. Then,

$$det(O) = \frac{-1}{C_A R_A} u_4.$$

In the literature, we call the observability singularity manifold or the unobservability submanifold the subset S given by

$$S = \left\{ z \in \mathrm{IR}^5 / \det[dh_1, dh_2, dL_f h_1, dL_f^2 h_1]^T = 0 \right\}$$

Then, for the cardiovascular systems considered we have:

$$S = \left\{ z \in \mathrm{IR}^5 / \frac{-1}{C_A R_A} u_4 = 0 \right\} = S_4.$$

when CVS evolves on S we lose the linear and nonlinear observability. Then,
(1) If $u_4 \neq 0$, then $rank(O) = 5$ and therefore we recover the quadratic observability of z_2^2.
(2) If $u_4 = 0$, then $rank(O) = 4$ and therefore we lose the observability of z_2^2.

2.3 Sliding mode observer design

In this subsection, we will present the observer structure that takes into account quadratic observability singularities due to either state separation or universal input. This method is based on the step-by-step sliding mode approach (Barbot et al. (2002), Floquet and Barbot (2007), Barbot and Floquet (2010)). We assume that the state z_1^1 and z_1^2 are directly measurable, but the others are not. The sliding mode observer is given by:

$$\begin{cases} \dot{\hat{z}}_1^1 = -\frac{R_C}{L_S} z_1^1 + \hat{z}_2^1 + \beta^{12} z_1^2 + \delta_1^1 sign\left(z_1^1 - \hat{z}_1^1\right) \\ \dot{\hat{z}}_2^1 = -\frac{1}{L_S C_S} z_1^1 + \hat{z}_3^1 + E_1^1 \delta_2^1 sign\left(\tilde{z}_2^1 - \hat{z}_2^1\right) \\ \dot{\hat{z}}_3^1 = \frac{1}{L_S R_S C_S^2} z_1^1 + \beta^{13} \tilde{z}_3^1 + k_{31}^{13} \tilde{z}_3^1 u_1 + k_{21}^{13} \tilde{z}_2^1 u_1 + k_{22}^{13} \tilde{z}_2^2 u_3 \\ \quad + E_2^1 \delta_3^1 sign\left(\tilde{z}_3^1 - \hat{z}_3^1\right) \\ \dot{\hat{z}}_1^2 = \beta^{21} z_1^1 - \frac{1}{C_A R_A}\left(z_1^2 u_2 + \hat{z}_2^2 u_4\right) + \delta_1^2 sign\left(z_1^2 - \hat{z}_1^2\right) \\ \dot{\hat{z}}_2^2 = k_{31}^{22} \tilde{z}_3^1 u_1 - \frac{L_S}{R_M} \tilde{z}_2^1 u_1 - \frac{1}{R_M} \tilde{z}_2^2 u_3 + \frac{1}{R_A} z_1^2 u_2 \\ \quad - \frac{1}{R_A} \tilde{z}_2^2 u_4 + E_1^2 \delta_2^2 sign\left(\tilde{z}_2^2 - \hat{z}_2^2\right) \end{cases} \tag{8}$$

In system (8) the auxiliary components $\tilde{z}_i$ are calculated algebraically as follows:

$$\begin{aligned} \tilde{z}_2^1 &= \hat{z}_2^1 + \delta_1^1 sign(z_1^1 - \hat{z}_1^1) \\ \tilde{z}_2^2 &= \hat{z}_2^2 + \frac{C_A R_A E_{SA}}{u_4 + E_{SA} - 1} E_1^2 \delta_1^2 sign(z_1^2 - \hat{z}_1^2) \\ \tilde{z}_3^1 &= \hat{z}_3^1 + \delta_2^1 sign(\tilde{z}_2^1 - \hat{z}_2^1) \text{ or} \\ \tilde{z}_3^1 &= \hat{z}_3^1 + \frac{1}{k_{31}^{22} u_1 + E_{SM} - 1} \delta_2^2 sign(\tilde{z}_2^2 - \hat{z}_2^2) \end{aligned}$$

with the following conditions:
if $\hat{z}_1^1 = z_1^1$ and $\hat{z}_1^2 = z_1^2$ then $E_1^1 = E_1^2 = 1$ otherwise $E_1^1 = E_1^2 = 0$,
if $\hat{z}_2^1 = z_2^1$ and $E_1^1 = E_1^2 = 1$ then $E_2^1 = 1$ otherwise $E_2^1 = 0$,
if $u_1 = 1$ then $E_{SM} = 1$ otherwise $E_{SM} = 0$,
if $u_4 = 1$ then $E_{SA} = 1$ otherwise $E_{SA} = 0$.

Now, we present the proof of the convergence of the observer (8). The study of the observer's stability and convergence uses equivalent vector methods (Drazenovic (1969)). The observer convergence strategy is carried out step by step on different sliding surfaces and ensures convergence of the observation error in 3 steps and in finite time to zero in the Lyapunov sense (Barbot et al. (2002), Floquet and Barbot (2007), Barbot and Floquet (2010)).

proof 2.1. The dynamics of the observer error ($e = z - \hat{z}$) is written:

$$\begin{aligned} \dot{e}_1^1 &= -\frac{R_C}{L_S} e_1^1 + e_2^1 + \beta^{12} e_1^2 - \delta_1^1 sign\left(z_1^1 - \hat{z}_1^1\right) \\ \dot{e}_2^1 &= -\frac{R_C}{L_S} e_1^1 + e_3^1 + E_1^1 \delta_2^1 sign\left(\tilde{z}_2^1 - \hat{z}_2^1\right) \\ \dot{e}_3^1 &= (\beta^{13} + k_{31}^{13} u_1) e_3^1 + k_{21}^{13} u_1 e_2^1 + k_{22}^{13} u_3 e_2^2 - E_2^1 \delta_3^1 sign\left(\tilde{z}_3^1 - \hat{z}_3^1\right) \\ \dot{e}_1^2 &= \beta^{21} e_1^1 - \frac{1}{C_A R_A} u_2 e_1^2 - \frac{1}{C_A R_A} e_2^2 u_4 + \delta_1^2 sign\left(z_1^2 - \hat{z}_1^2\right) \\ \dot{e}_2^2 &= k_{31}^{22} e_3^1 u_1 - \frac{L_S}{R_M} e_2^1 u_1 - \frac{1}{R_M} e_2^2 u_3 + \frac{1}{R_M} e_1^2 u_2 - \frac{1}{R_M} e_2^2 u_4 \\ &\quad + E_1^2 \delta_2^2 sign\left(\tilde{z}_2^2 - \hat{z}_2^2\right) \end{aligned}$$

• **Step 1:** Assume $z_1^1(0) \neq \hat{z}_1^1(0)$ and $z_1^2(0) \neq \hat{z}_1^2(0)$ and as $E_1^1 = E_2^1 = E_1^2 = 0$ in the first step, we obtain the following observation error dynamics:

$$\begin{cases} \dot{e}_1^1 = -\frac{R_C}{L_S} e_1^1 + e_2^1 + \beta^{12} e_1^2 - \delta_1^1 sign\left(z_1^1 - \hat{z}_1^1\right) \\ \dot{e}_2^1 = -\frac{R_C}{L_S} e_1^1 + e_3^1 \\ \dot{e}_3^1 = (\beta^{13} + k_{31}^{13} u_1) e_3^1 + k_{21}^{13} u_1 e_2^1 + k_{22}^{13} u_3 e_2^2 \\ \dot{e}_1^2 = \beta^{21} e_1^1 - \frac{u_2}{C_A R_A} e_1^2 - \frac{u_4}{C_A R_A} e_2^2 + \delta_1^2 sign\left(z_1^2 - \hat{z}_1^2\right) \\ \dot{e}_2^2 = k_{31}^{22} e_3^1 u_1 - \frac{L_S}{R_M} e_2^1 u_1 - \frac{u_3}{R_M} e_2^2 + \frac{u_2}{R_M} e_1^2 - \frac{u_4}{R_M} e_2^2 \end{cases}$$

Let $S_1 = \{e_1^1 = e_1^2 = 0\}$ be the sliding surface and the Lyapunov function $V_1^1 = \frac{(e_1^1)^2}{2}$ and $V_1^1 = \frac{(e_1^2)^2}{2}$. The sliding surface is attractive if and only if $\dot{V}_1^1 = e_1^1 \dot{e}_1^1 < 0$ and $\dot{V}_1^2 = e_1^2 \dot{e}_1^2 < 0$, then

$$e_1^1 \left(-\frac{R_C}{L_S} e_1^1 + e_2^1 + \beta^{12} e_1^2 - \delta_1^1 sign\left(z_1^1 - \hat{z}_1^1\right) \right) < 0 \text{ and}$$

$$e_1^2 \left(\beta^{21} e_1^1 - \frac{u_2}{C_A R_A} e_1^2 - \frac{u_4}{C_A R_A} e_2^2 + \delta_1^2 sign\left(z_1^2 - \hat{z}_1^2\right) \right) < 0$$

By choosing, $\delta_1^1 > \left\| e_2^1 \right\|_{\max}$ and $\delta_1^2 > \left\| e_2^2 \right\|_{\max}$, there exists a finite time $\tau_1 \geqslant 0$ such that $\forall t \geqslant \tau_1$ we have $\hat{z}_1^1 = z_1^1$, $\hat{z}_1^2 = z_1^2$ and $E_1^1 = E_1^2 = 1$. Then $\dot{e}_1^1 = \dot{e}_1^2 = 0$. Therefore

$$\tilde{z}_2^1 = \hat{z}_2^1 + \delta_1^1 sign\left(z_1^1 - \hat{z}_1^1\right) \quad \text{and}$$
$$\tilde{z}_2^2 = \hat{z}_2^2 + \frac{C_A R_A}{u_4} E_1^2 \delta_1^2 sign\left(z_1^2 - \hat{z}_1^2\right)$$

So we can see that when $u_4 = 0$, $\tilde{z}_2^2$ tends to infinity, meaning that observability singularity occurs. Thus, to avoid the explosion of z_2^2 we introduce a E_{SA} as follows: If $u_4 = 0$ then $E_{SA} = 0$ otherwise $E_{SA} = 1$. Then $\tilde{z}_2^2$ becomes:

$$\tilde{z}_2^2 = \hat{z}_2^2 + \frac{C_A R_A E_{SA}}{u_4 + E_{SA} - 1} E_1^2 \delta_1^2 sign\left(z_1^2 - \hat{z}_1^2\right)$$

And consequently, by choosing, $\delta_1^1 > \left\|e_2^1\right\|_{\max}$ and $\delta_1^2 > \left\|e_2^2\right\|_{\max}$, there exists a finite time $\tau_1 \geqslant 0$ such that $\forall t \geqslant \tau_1$ we have $\dot{e}_1^1 = \dot{e}_1^2 = 0$ and $\tilde{z}_2^1 = z_2^1$ and $\tilde{z}_2^2 = z_2^2$.

• **Second Step:** The aim of this step is to reach $e_1^1 = e_1^2 = 0$. So $\forall t \geqslant \tau_1$, we have $\tilde{z}_2^1 = z_2^1$ and $\tilde{z}_2^2 = z_2^2$.
As $\hat{z}_1^1 = z_1^1$ and $\hat{z}_1^2 = z_1^2$ then $E_1^1 = 1$, $E_1^2 = 1$ then $e_1^1 = 0$ and $e_1^2 = 0$ for all $t \geq \tau_1$ then $\dot{e}_1^1 = 0$ and $\dot{e}_2^2 = 0$ then consequently, invoking the equivalent vector, $\tilde{z}_2^1 = z_2^1$ and $\tilde{z}_2^2 = z_2^2$, we obtain:

$$\begin{aligned}
\dot{e}_1^1 &= 0 \\
\dot{e}_2^1 &= e_3^1 + \delta_2^1 sign\left(\tilde{z}_2^1 - \hat{z}_2^1\right) \\
\dot{e}_3^1 &= (\beta^{13} + k_{31}^{13} u_1) e_3^1 \\
\dot{e}_1^2 &= 0 \\
\dot{e}_2^2 &= k_{31}^{22} e_3^1 u_1 + \delta_2^2 sign\left(\tilde{z}_2^2 - \hat{z}_2^2\right)
\end{aligned}$$

To do this, let's pose the Lyapunov function:
$V_2^1 = \frac{(e_1^1)^2}{2} + \frac{(e_2^1)^2}{2}$ and $V_2^2 = \frac{(e_1^1)^2}{2} + \frac{(e_2^2)^2}{2}$. The sliding surface $S_2 = \left\{e_1^1 = e_2^1 = e_1^2 = e_2^2 = 0\right\}$ is attractive if and only if

$$\dot{V}_2^1 = e_2^1 \dot{e}_2^1 = e_2^1 \left(e_3^1 + \delta_2^1 sign\left(\tilde{z}_2^1 - \hat{z}_2^1\right)\right) < 0 \text{ and}$$
$$\dot{V}_2^2 = e_2^2 \dot{e}_2^2 = e_2^2 \left(k_{31}^{22} e_3^1 u_1 + \delta_2^2 sign\left(\tilde{z}_2^2 - \hat{z}_2^2\right)\right) < 0$$

By choosing, $\delta_2^1 > \left\|e_3^1\right\|_{\max}$ and $\delta_2^2 > \left\|e_3^1\right\|_{\max}$, there exists a finite time $\tau_2 \geq \tau_1 \geq 0$ such that $\forall t \geq \tau_2$, we have $\hat{z}_2^1 = z_2^1$, $\hat{z}_2^2 = z_2^2$ and $E_1^1 = E_1^2 = E_1^1 = E_2^1 = 1$. Then $\dot{e}_2^1 = \dot{e}_2^2 = 0$. Therefore

$$\tilde{z}_3^1 = \hat{z}_3^1 + \delta_2^1 sign\left(\tilde{z}_2^1 - \hat{z}_2^1\right) \text{ or}$$
$$\tilde{z}_3^1 = \hat{z}_3^1 + \frac{1}{k_{31}^{22} u_1} \delta_2^2 sign\left(\tilde{z}_2^2 - \hat{z}_2^2\right)$$

Due to the finite time convergence of the sliding mode, there exists $\tau_2 > \tau_1 > 0$ such that $\forall t \geq \tau_2$, $\hat{z}_2^1 = \tilde{z}_2^1 = z_2^1$ and $\hat{z}_2^2 = \tilde{z}_2^2 = z_2^2$ then we pass to the:

• **Third Step:** The aim of this step is to reach $e_1^1 = e_2^1 = e_1^2 = e_2^2 = 0$. So $\forall t \geqslant \tau_2$, we have $\tilde{z}_3^1 = z_3^1$.
As $\hat{z}_1^1 = z_1^1$, $\hat{z}_2^1 = z_2^1$, $\hat{z}_1^2 = z_1^2$ and $\hat{z}_2^2 = z_2^2$ then $E_1^1 = E_1^2 = E_1^1 = 1$, then consequently, invoking the equivalent vector, $\tilde{z} = z$, we obtain:

$$\begin{aligned}
\dot{e}_1^1 &= \dot{e}_2^1 = 0 \\
\dot{e}_3^1 &= -\delta_3^1 sign\left(\tilde{z}_3^1 - \hat{z}_3^1\right) \\
\dot{e}_1^2 &= \dot{e}_2^2 = 0
\end{aligned}$$

Let $S_3 = \left\{e_1^1 = e_2^1 = e_3^1 = e_1^2 = e_2^2 = 0\right\}$ be the sliding surface and the Lyapunov function $V_3^1 = \frac{(e_1^1)^2}{2} + \frac{(e_2^1)^2}{2} + \frac{(e_3^1)^2}{2}$. The sliding surface is attractive if and only if

$$\dot{V}_3^1 = e_3^1 \dot{e}_3^1 = e_3^1 \left(-\delta_3^1 sign\left(\tilde{z}_3^1 - \hat{z}_3^1\right)\right) < 0$$

Then e_3^1 converges to 0 in a finite time $\tau_3 > \tau_2$ for any value of $\delta_3^1 > 0$ and if all conditions δ_1^1 , δ_2^1, δ_1^2 and δ_2^2 are satisfied after τ_2.

3. CVS MODEL FOR DETECTION OF ANOMALIES AND SIMULATIONS

In this sections, we consider faults in the inputs D_M and D_A for detecting anomalies in the mitral and aortic valves. As described before, the valves are a inputs vector can only have 0 or 1, this represents the ideal opening and closing of the mitral and aortic valves. However, there are cases when a valve either does not close completely or does not open fully. This medical terms to refer to these situations are valve regurgitation (faulty closing) and valve stenosis (faulty opening). Now, we propose to adapt the model (3) by including the following fault vector F which describe variations acting on the mitral valve f_m and f_{ao} aortic. The fault vector is given by following equation:

$$F(t) = \begin{bmatrix} f_m \\ f_{ao} \end{bmatrix}, \text{such as: } \begin{cases} U_1 = D_M + f_m \\ U_2 = D_A + f_{ao} \end{cases} \tag{9}$$

where D_M and D_A are the nominal values of the real state of the mitral valve and aortic valve, f_m and f_{ao} are the faults corresponding to the mitral and aortic valves respectively. The fault model of the SCV has the following form:

$$\begin{cases}
\dot{x}_1 &= \frac{-\dot{C}(t)}{C(t)} x_1 - \frac{U_1}{C(t) R_M}(x_1 - x_2) - \frac{U_2}{C(t) R_A}(x_1 - x_4) \\
\dot{x}_2 &= \frac{1}{R_S C_R}(x_3 - x_2) + \frac{1}{C_R R_M}(x_1 - x_2) U_1 \\
\dot{x}_3 &= \frac{1}{R_S C_S}(x_2 - x_3) + \frac{1}{C_S} x_5 \\
\dot{x}_4 &= -\frac{1}{C_A} x_5 + \frac{1}{C_A R_A}(x_1 - x_4) U_2 \\
\dot{x}_5 &= -\frac{1}{L_S} x_3 + \frac{1}{L_S} x_4 - \frac{R_C}{L_S} x_5
\end{cases} \tag{10}$$

Remark 3.1. In observer design, U_1 and U_2 are considered as bounded unknown inputs (Barbot et al. (2002)).

Simulations: Parameter values are (Simaan (2008)): $C_S = 1.33, C_R = 4.40, R_S = 1$, $C_A = 0.08, L_S = 0.0005$, $R_C = 0.0398, R_M = 0.005$ and R_A=0.001. For the initial conditions, we put $x_n = [0, -12e^4, 6.0150e^4, 60, 183.3]^T$ and $\hat{z}_n = [5, -11e^4, 5.7143e^4, 0, 150]^T$. Figures 2 to 3 illustrate the effectiveness of the choice of E_{SA} and E_{SM} for the good estimation z_1^1, z_2^1, z_3^1, z_1^2 and z_2^2. We can see that from the transformation presented in 4 we can obtain the estimated states $\hat{x}_2$ and $\hat{x}_3$ from the measurable outputs. In Figure 2, we assume that $E_{SA} = 0$ if $u_4 = 0$ and $E_{SM} = 0$ if $u_3 = 0$. This choice ensures that state estimation is completed within a finite time. Figure 3 presents the states of systems (3) and the observer (8). It demonstrates how the state estimation converges completely for all states within a time frame of 1.5 s. We observe that the convergence of the $\hat{z}_2^2$ state of the observer to z_2^2 of the system is dependent on the selection of E_{S_A} and E_{S_M}. To recover all the information of the unobservable state x_1, it is crucial to make appropriate choices for E_{S_A} and E_{S_M} in order to avoid information loss during estimation caused by the singularity formation of u_1 and u_2.

Remark 3.2. The simulations results show that the proposed sliding mode observer is more robust than the Kalman Filter proposed in (Diaz Ledezma and Laleg-Kirati (2015)).

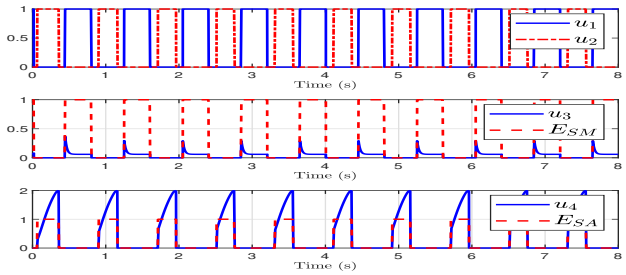

Fig. 2. States of u_3, E_{SM}, u_4 and E_{SA}

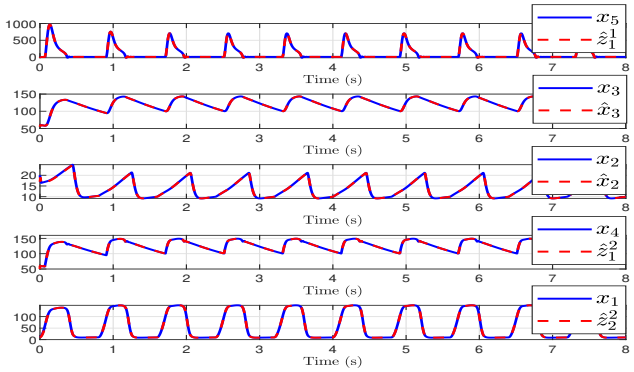

Fig. 3. States of the system and the observer

In the following two different scenarios of faults are given, the scenario 1 is mitral regurgitation and the scenario 2 is mitral regurgitation.

3.1 Case 1: Mitral Regurgitation

In this case, we consider a 50% regurgitation in the mitral valve (i.e. $f_m = 0.5$ when $u_1 = 0$ and $f_{ao} = 0$). The simulation of fault in the mitral valve was modeled as an addition to the valve (1 or 0) of the input u_1. This change was introduced at time $t = 2.5s$. In figure 4, we can see that after the fault occurs in the mitral valve, there is a change in the aortic valve, u_3 and u_4 have a change in the dynamics because they depend on u_1 and u_2. In figure 5, we can see the change in the dynamics system when the failure occurs, blood flow decreases and pressures change. Also, we show that the SMO can adapt to the change in the dynamics, also the observer can reconstruct the unobservable state when the failure occurs, but only states x_3, x_4 and x_5 are able to convergent again to the true state.

3.2 Case 2: Aortic Regurgitation

In this case, we consider a 50% regurgitation in the aortic valve (i.e. $f_{ao} = 0.5$ when $u_2 = 0$ and $f_m = 0$). The simulation of fault in the aortic valve was modeled as an addition to the valve (1 or 0) of the input u_2. This change was introduced at time $t = 2.5s$. In the figure 6, we can see that after the fault occurs in the aortic valve, there is a change in the mitral valve, also u_3 and u_4 have a change in the dynamics because they depend of u_1 and u_2. In the figure 7, we can see the change the dynamics system when the failure occurs, blood flow the blood flow changes and pressures increase. However, we show that the SMO has the capacity to adapt to the change in the dynamics, also the observer is able to reconstruct the unobservable state when the failure occurs, but only states x_3, x_4 and x_5 can convergent again to the true state and the state x_1 and x_2 have a constant error.

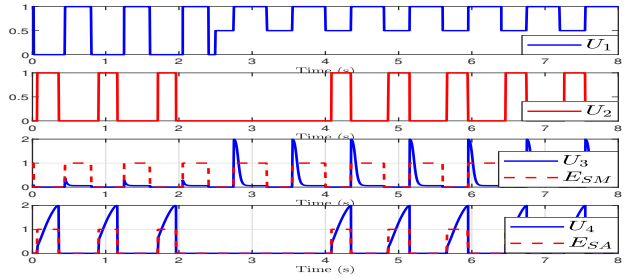

Fig. 4. States of inputs with fault f_m

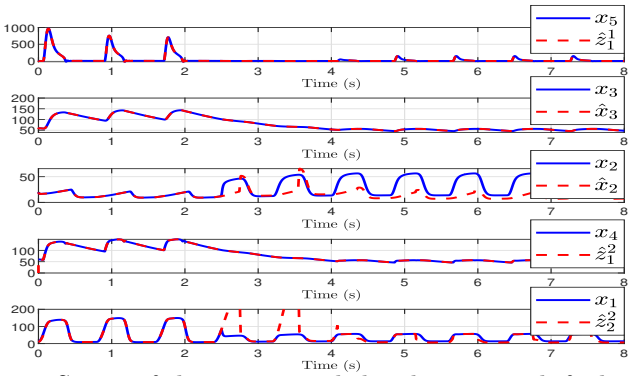

Fig. 5. States of the system and the observer with fault

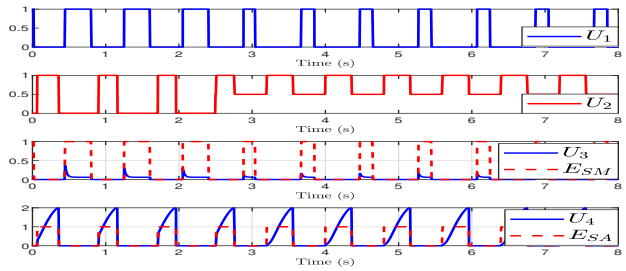

Fig. 6. States of input with fault f_{ao}

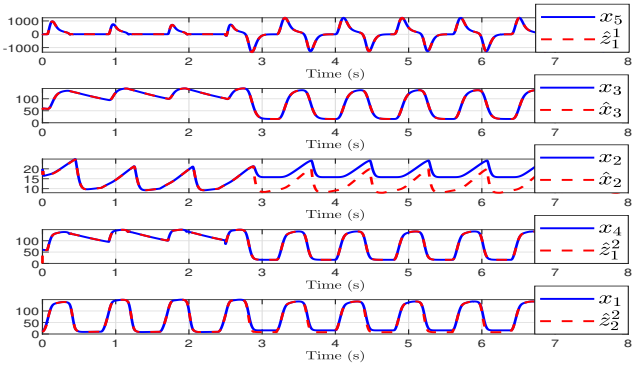

Fig. 7. States of the system and the observer with fault

4. CONCLUSION

In this paper, the detection of cardiovascular dysfunctions or anomalies using sliding-mode observers is presented. To this end, we first analyzed observability for a nonlinear cardiovascular model. Then, we proposed a sliding-mode observer that allowed us to recover observability, despite the fact that the cardiovascular model is not linearly observable. Moreover, the singularities of observability are taken into account in the construction of the sliding-mode observer. Finally, two cases of mitral and aortic valve failure are considered, representing a cardiac problem (valvular regurgitation), and we can observe that the observer can reconstruct the dynamics of the unobservable state.

ACKNOWLEDGEMENTS

We would like to thank the CONACYT for the financial support for the project named SUSTAINABILITY AND AUTOMATIC CONTROL with the number 000000000320056.

REFERENCES

Barbot, J.P. and Floquet, T. (2010). Iterative higher order sliding mode observer for nonlinear systems with unknown inputs. *Dynamics of Continuous, Discrete and Impulsive Systems*, 1019–1033, vol.17.

Barbot, J., Boukhobza, T., and Djemai, M. (2002). Sliding mode observer for triangular input form. In *Proceedings of 35th IEEE Conference on Decision and Control*, 1489–1490 vol.2.

Belkhatir, Z., Laleg-Kirati, T.M., and Tadjine, M. (2014). Residual generator for cardiovascular anomalies detection. In *2014 European Control Conference (ECC)*, 1862–1868.

Boutat-Baddas, L. (2002). *Analyse des singularités d'observabilité et de détectabilité: Application à la synchronisation des circuits éléctroniques chaotiques*. Ph.D. thesis, Cergy-Pontoise.

Brunovskỳ, P. (1970). A classification of linear controllable systems. *Kybernetika*, 173–188, vol. 6.

Diaz Ledezma, F. and Laleg-Kirati, T.M. (2015). A first approach on fault detection and isolation for cardiovascular anomalies detection. In *2015 American Control Conference (ACC)*, 5788–5793.

Drakunov, S. and Utkin, V. (1995). Sliding mode observers. tutorial. In *Proceedings of 1995 34th IEEE Conference on Decision and Control*, 3376–3378 vol.4.

Drakunov, S. (1992). Sliding-mode observers based on equivalent control method. In *Proceedings of the 31st IEEE Conference on Decision and Control*, 2368–2369 vol.2.

Drazenovic, B. (1969). The invariance conditions in variable structure systems. *Automatica*, 287–295.

Ferreira, A., Chen, S., Simaan, M.A., Boston, J.R., and Antaki, J.F. (2005). A nonlinear state-space model of a combined cardiovascular system and a rotary pump. In *Proceedings of the 44th IEEE Conference on Decision and Control*, 897–902. IEEE.

Floquet, T. and Barbot, J.P. (2007). Super twisting algorithm-based step-by-step sliding mode observers for nonlinear systems with unknown inputs. *International Journal of Systems Science*, 803–815 vol.38.

Fónod, R. and Krokavec, D. (2012). Actuator fault estimation using neuro-sliding mode observers. In *2012 IEEE 16th International Conference on Intelligent Engineering Systems (INES)*, 405–410.

Korakianitis, T. and Shi, Y. (2006). A concentrated parameter model for the human cardiovascular system including heart valve dynamics and atrioventricular interaction. *Medical engineering & physics*, 613–628, vol.28.

Krener, A.J. and Isidori, A. (1983). Linearization by output injection and nonlinear observers. *Systems & Control Letters*, 47–52, vol. 3.

Laleg-Kirati, T.M., Belkhatir, Z., and Ledezma, F.D. (2015). Application of hybrid dynamical theory to the cardiovascular system. *Hybrid Dynamical Systems: Observation and Control*, 315–328.

Ledezma, F.D. and Laleg-Kirati, T.M. (2012). Detection of cardiovascular anomalies: Hybrid systems approach. *4th IFAC Conference on Analysis and Design of Hybrid Systems*, 222–227, vol. 45.

Organization, W.H. (June 2023). www.who.int/health-topics/cardiovascular-diseases #tab=tab_1.

Serrano-Cruz, D.A., Boutat-Baddas, L., Darouach, M., and Astorga-Zaragoza, C.M. (2021). Observer design for a nonlinear cardiovascular system. In *2021 9th International Conference on Systems and Control (ICSC)*, 294–299. IEEE.

Simaan, M.A. (2008). Modeling and control of the heart left ventricle supported with a rotary assist device. In *2008 47th IEEE Conference on Decision and Control*, 2656–2661. IEEE.

Simaan, M.A., Ferreira, A., Chen, S., Antaki, J.F., and Galati, D.G. (2008). A dynamical state space representation and performance analysis of a feedback-controlled rotary left ventricular assist device. *IEEE Transactions on Control Systems Technology*, 15–28, vol. 17.

Traver, J.E., Nuevo-Gallardo, C., Tejado, I., Fernández-Portales, J., Ortega-Morán, J.F., Pagador, J.B., and Vinagre, B.M. (2022). Cardiovascular circulatory system and left carotid model: A fractional approach to disease modeling. *Fractal and Fractional*, 6.

Utkin, V. (1977). Variable structure systems with sliding modes. *IEEE Transactions on Automatic Control*, 212–222, vol.22.

Utkin, V.I. (1992). *Sliding modes in control and optimization*. Springer Science & Business Media.

Xiao, H., Butlin, M., Qasem, A., Tan, I., Li, D., and Avolio, A.P. (2018). N-point moving average: A special generalized transfer function method for estimation of central aortic blood pressure. *IEEE Transactions on Biomedical Engineering*, 1226–1234, vol. 65.

Y. Shtessel, C. Edwards, L.F. and Levant, A. (2014). Sliding mode control and observation.

Émile S. Kenny, J. (2021). Functional hemodynamic monitoring with a wireless ultrasound patch. *Journal of Cardiothoracic and Vascular Anesthesia*, 1509–1515, vol. 35.